Smart Building: Use of the Artificial Neural Network Approach for Indoor Temperature Forecasting

Nivine Attoue [1], Isam Shahrour [1,2,*] and Rafic Younes [3]

[1] Laboratory of Civil Engineering and Geo-Environment, Lille University, 59650 Villeneuve d'Ascq, France; nivine.attoue@gmail.com
[2] School of Civil Engineering, Tongji University, Shanghai 200092, China
[3] Modeling Center, Lebanese University, Hadath 99000, Lebanon; ryounes@ul.edu.lb
[*] Correspondence: isam.shahrour@univ-lille1.fr; Tel.: +33-320434545

Abstract: The smart building concept aims to use smart technology to reduce energy consumption, as well as to improve comfort conditions and users' satisfaction. It is based on the use of smart sensors and software to follow both outdoor and indoor conditions for the control of comfort, and security devices for the optimization of energy consumption. This paper presents a data-based model for indoor temperature forecasting, which could be used for the optimization of energy device use. The model is based on an artificial neural network (ANN), which is validated on data recorded in an old building. The novelty of this work consists of the methodology proposed for the development of a simplified model for indoor temperature forecasting. This methodology is based on the selection of pertinent input parameters after a relevance analysis of a large set of input parameters, including solar radiation outdoor temperature history, outdoor humidity, indoor facade temperature, and humidity. It shows that an ANN-based model using outdoor and facade temperature sensors provides good forecasting of indoor temperatures. This model can be easily used in the optimal regulation of buildings' energy devices.

1. Introduction

The smart building concept aims to use smart technology to reduce energy consumption, as well as to improve comfort and users' satisfaction. Forecasting of the indoor temperature is necessary for the regulation of energy devices to ensure occupant comfort, as well as for energy optimization [1,2]. This forecasting constitutes a complex task, because it is governed by complex physical and behavioral phenomena. It is affected by a multitude of parameters, which could be classified into three groups: outdoor conditions, building characteristics, and occupants' behavior [3–5]. In addition, investigations showed that the indoor temperature does not have uniform distribution [6].

Indoor temperature forecasting could be carried out using physical or data-driven approaches [7]. The physical approach is based on the use of numerical modelling [8,9], which requires detailed information about a building's characteristics, appliances, and occupant behavior.

The data-driven approach is based on the use of collected data for developing relationships (models) between 'input' parameters and 'output' parameters. These relationships could be established by learning from collected data. The artificial neural network (ANN) approach was used to build data-driven models [10–12]. Soleimani-Mohseni et al. [13] showed that the operative temperature could be well estimated by the ANN approach using the indoor air temperature, electrical power, outdoor temperature, time of day, wall temperature, and ventilation flow rate. Lu and Viljanen [14]

used the ANN approach to predict air temperature and relative humidity in a test room using indoor and outdoor temperature and humidity. Recently, Zabada and Shahrour [15] used the ANN approach for the analysis of the heating expenses in social housing. In these works, the ANN model was used as a prediction tool for specific cases. This paper proposes a methodology, which could be followed for the use of the ANN approach for the indoor temperature forecasting in any type of building. This methodology is based on the use of a relevance analysis for the determination of pertinent input parameters and the optimal ANN architecture. The methodology is presented through its application on data recorded in an old building.

2. Data Collection

Data were collected using a smart monitoring of an old building of Polytech'Lille Engineering School in the north of France. Monitoring concerned indoor and outdoor temperature and humidity, as well as solar radiation [16,17]. Parameters were recorded at five-minute intervals and then sent to a local server. Figure 1 illustrates an example of recorded data on a summer day. Data concerns the outdoor temperature, as well as the indoor temperature at three locations in the office: facade, center of the lateral wall, and office center. The external temperature varied between 17.5 °C and 34 °C, while the facade indoor temperature varied between 21 °C and 25.5 °C. The temperatures at the center of the office and the center of the lateral wall varied between 22 °C and 24.2 °C.

Data were collected for two summer months (June and July) in different offices of the building.
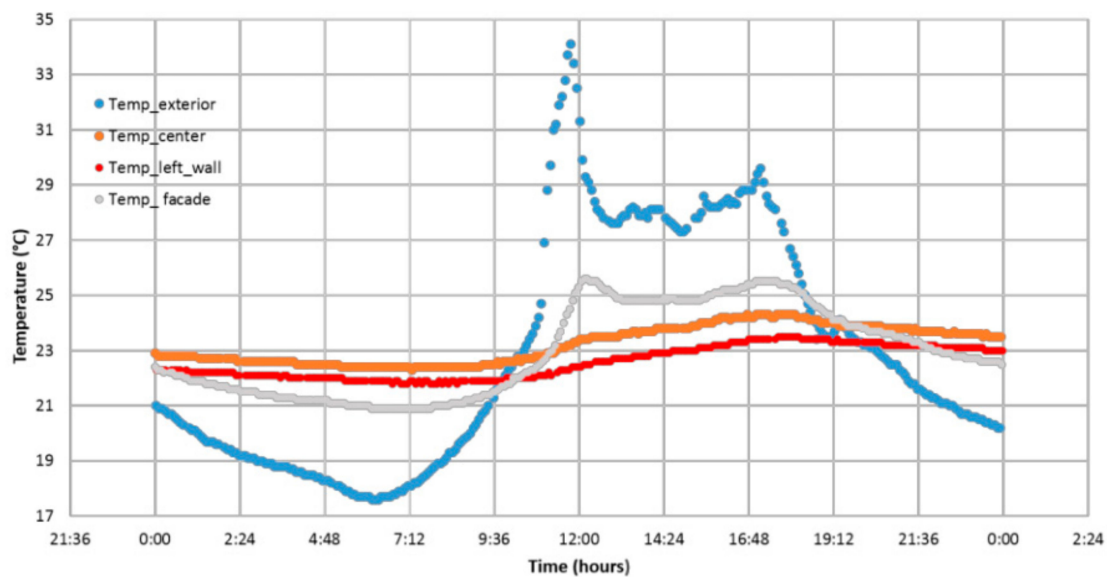

Figure 1. Temperature variation on a summer day.

3. Artificial Neural Network Approach

The ANN approach is inspired from the ability of the human brain to predict patterns based on learning and recalling processes. It allows the construction of relationships between input parameters and output parameters using artificial neurons, which are arranged in an input layer, an output layer and one or more hidden layers [18]. Analyses were conducted using the multilayer back-propagation neural network. We used a three-layer ANN with n, m, and k as the number of input, hidden, and output nodes, respectively, based on the equation:

$$Y_k = S(\sum_{j=1}^{m} W_{jk} \times S(\sum_{i=1}^{n} W_{ij}X_i)), \tag{1}$$

where Y_k stands for the output values and X_i denotes the input values; W_{ij} gives the weights of connection between the input layer and the hidden layer.

The ANN performances could be evaluated using the mean square error (*MSE*) and the coefficient of correlation (*R*)

$$MSE = \sum_{i=1}^{n} \left(\frac{e_i^2}{N} \right),$$ (2)

$$R = \pm \sqrt{\frac{\sum_{i=1}^{N} (Y_i - \overline{X})^2}{\sum_{i=1}^{N} (X_i - \overline{X})^2}} = \sqrt{1 - \frac{\sum_{i=1}^{N} (e_i)^2}{\sum_{i=1}^{N} (X_i - \overline{X})^2}}$$ (3)

where e_i is the error between the ANN output (Y_i) and the experimental input (X_i), $\overline{X}$ represents the mean of the input target.

Different ANN architectures exist. The multilayer perception (MLP) structure is the most popular [19–24]. Its use with a single hidden layer and a sufficient number of neurons provided good accuracy for the approximated function [25,26]. This architecture is used in this work.

The use of ANN for temperature forecasting aims to predict the building indoor temperature for the optimal regulation of energy devices as well as for ensuring occupants' comfort. Indoor conditions of a building are highly affected by its age and thermal performance, which depends on its envelope and construction material. The input parameters concern the outdoor conditions, indoor conditions, as well as the occupants' behavior. The forecasting time depends on the building thermal inertia and energy regulation system. Each building is characterized by its time lag and the time of heat transmission delay [27–30]. The prediction time for ANN models ranged from 0.5 to 4 h to cover the phase of heating exchange through the facade and to investigate the effectiveness of this approach.

This paper proposes a methodology composed of two steps for the use of the ANN approach for indoor temperature forecasting. The first step concerns the indoor facade temperature forecasting considering outdoor and indoor conditions, while the second step concerns the prediction of the temperature at the room center considering the indoor facade temperature.

Analyses were conducted using MATLAB (Mathworks Inc., Natick, MA, USA—Group License) for ANN modeling and IBM SPSS statistics for input parameter ranking.

4. Facade Indoor Temperature Forecasting

4.1. Analysis of the Input Parameters' Relevance

The input parameters used in the global analysis are summarized in Table 1. They concern the outdoor conditions (temperature, humidity, and solar radiation), outdoor temperature history (input matrix for the last 3-h values having 30 min lag between its different columns: if the actual outdoor temperature was recorded at time t, the history matrix corresponds to t—0.5 h, t—1 h, t—1.5 h, t—2 h, t—2.5 h, and t—3 h, the indoor facade temperature history (similar matrix history as the outdoor temperature), and time (cumulative minutes of the day). The time range of history inputs was chosen with respect to the prediction time to cover the phase shift that will occur at the facade level. The impact of a larger range (t—5 h, t—6 h, etc.) for the history inputs did not affect the results. A 30 min lag was chosen to detect any sudden variation at the facade level.

Table 1. Input parameters for the facade temperature forecasting.

Input Parameters
Outdoor temperature
Outdoor humidity
Solar radiation
Outdoor temperature history
Time
Facade temperature history

The ANN optimal architecture (Figure 2) was fixed after several comparative analyses. It includes one hidden layer with four neurons. Table 2 provides the weights of neurons' connections obtained from MATLAB software. We can observe that the weight could be negative or positive providing excitatory or inhibitory influence on each input.
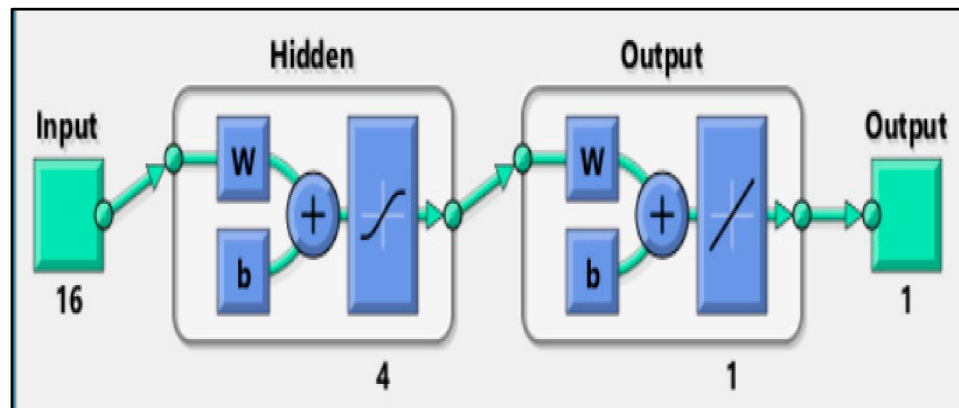

Figure 2. Artificial Neural Network (ANN) optimal architecture.

Table 2. Weight of neurons' connections.

Input Parameters	Neuron 1	Neuron 2	Neuron 3	Neuron 4
Time	2.59	0.02	1.46	−0.02
Outdoor temperature	1.13	−1.25	−0.05	1.32
History of outdoor temperature	2.55	1.65	−0.93	−1.60
	1.79	−1.05	−1.66	0.93
	2.67	0.62	−2.02	−0.64
	−1.11	−0.95	0.17	0.92
	−1.21	0.21	−0.54	−0.27
	0.86	−0.02	0.23	0.06
History of facade temperature	−2.65	−0.72	−2.76	1.43
	−3.00	0.90	−1.58	−1.12
	−1.04	0.50	−1.20	−0.38
	−0.26	0.61	−1.18	−0.57
	0.50	−0.31	−0.13	0.33
	−0.34	0.07	−1.10	−0.12
Solar radiation	1.27	0.23	3.52	−0.22
Outdoor humidity	0.01	−0.10	−0.43	0.09

Figure 3 shows comparison of 'predicted' and 'recorded' facade temperatures. We observe a good agreement between these values with $R = 0.9967$ and $MSE = 0.0277$. This result shows that the ANN model predicts well the facade indoor temperature. The determination of input parameters requires two temperature sensors (outdoor and indoor), an external humidity sensor, and a solar radiation sensor.
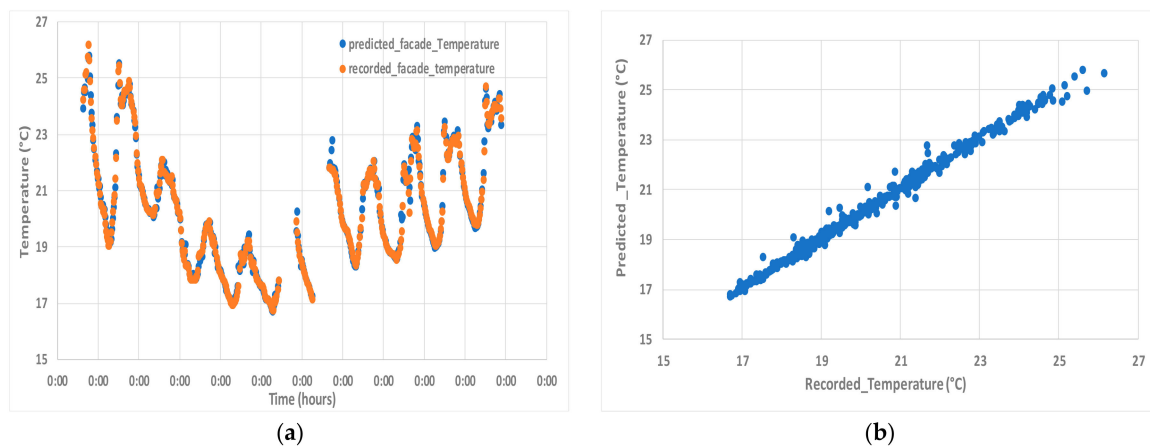
Figure 3. Predicted and recorded facade temperatures: (**a**) variation of both temperatures in time domain; and (**b**) the predicted facade temperature with the recorded facade temperature.

In order to determine the most important input parameters in the ANN model, IBM SPSS statistical software was used to analyze the 'importance' of these parameters. This software is based on inferential statistics. It uses recorded data to perform a sensitivity analysis for the determination of the importance of each input parameter. Table 3 summarizes the obtained results. It shows that the solar radiation, time and humidity have a low role in the forecasting model, with an importance factor lower than 5.1%. The outdoor temperature has the highest importance (Importance Factor = 42%), followed by the historical facade temperature (Importance Factor = 31.9%). The historical outdoor temperature has an intermediate influence with an Importance Factor = 12.8%.

Table 3. Analysis of the relevance of input parameters.

Parameter	Importance Factor (%)
Solar radiation	3.7
Time	4.5
Humidity	5.1
Historic outdoor temperature	12.8
Historic facade temperature	31.9
Outdoor temperature	42.0

Since the role of some input parameters in the ANN model is very weak (with reference to the SPSS classification), analyses were conducted by neglecting these parameters. Table 4 summarizes the results of these analyses. It shows clearly that the neglect of solar radiation, humidity, and historical outdoor temperature (Model 5) does not significantly deteriorate the quality of the ANN model: the mean square error (*MSE*) increases from 0.0277 to 0.0365, while the coefficient of correlation (*R*) decreases from 0.9967 to 0.9959. The additional neglect of the historical data of the facade temperature (Model 6) has a higher influence: *MSE* increases from 0.0277 to 0.4922, while R decreases from 0.9967 to 0.946. Figure 4 illustrates the results of Models 1, 5, and 6. As expected and according to the physics of the heat transfer in transient conditions, this result shows that the facade temperature could be effectively predicted in considering only the outdoor temperature and the historical data of the facade indoor temperature.
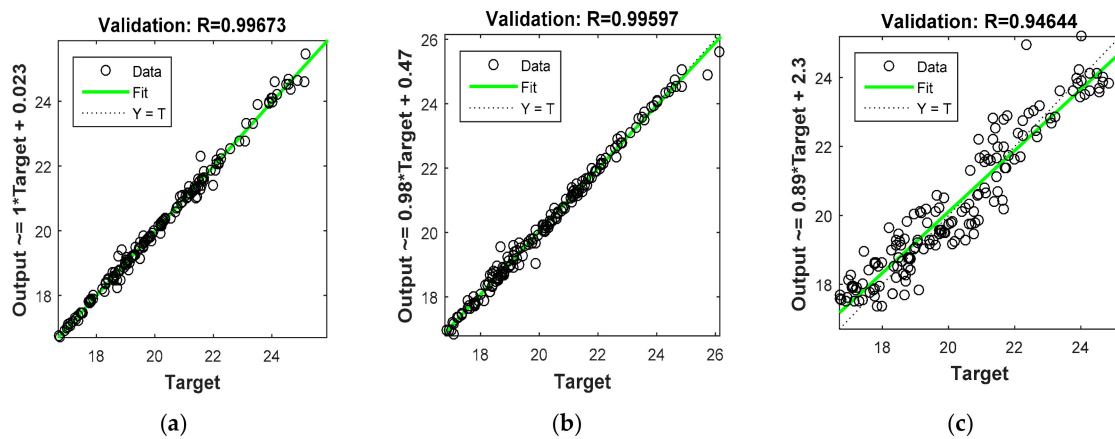
Figure 4. *R* results for different models: (**a**) Model 1; (**b**) Model 5; and (**c**) Model 6.

Table 4. Degraded model results.

| Model	Input Parameter	R	MSE
1	Outdoor temperature and history, outdoor humidity, sun radiation, time, facade history	0.9967	0.0277
2	Outdoor temperature, historic, outdoor humidity, time, facade history	0.99687	0.03
3	Outdoor temperature, historic, outdoor humidity, facade history	0.9969	0.0269
4	Outdoor temperature, historic, facade history	0.9975	0.0199
5	Outdoor temperature, facade history	0.9959	0.0365
6	Outdoor temperature	0.946	0.4922

4.2. Facade Temperature Forecasting Model

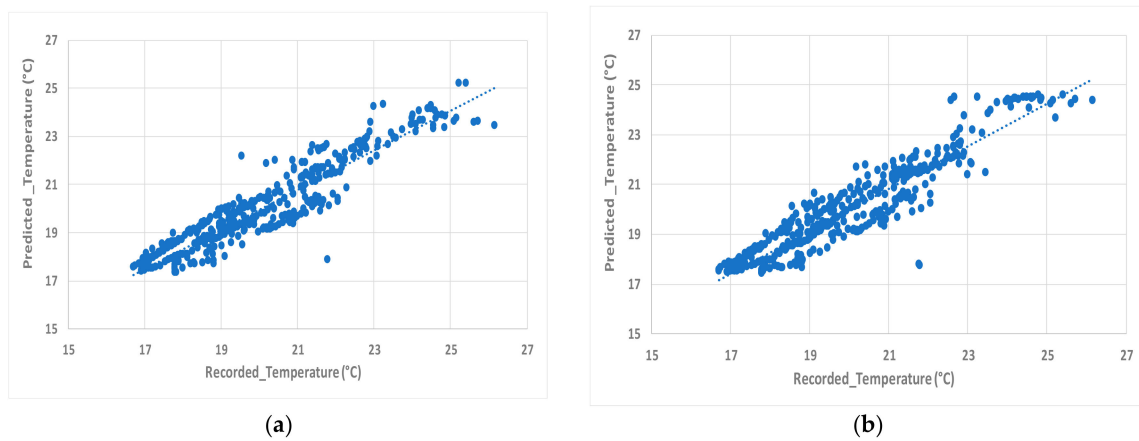#### 4.2.1. Use of the Outdoor Temperature as Input Parameter

Considering the results of the previous section, the outdoor temperature is first used as the input parameter for forecasting the facade indoor temperature. The forecasting model provides the temperature at 0.5, 1, 2, and 4 h.

Figures 5 and 6 show the forecasting results at 0.5 and 1.0 h. We observe that the ANN model reproduces well the recorded temperature. For 0.5-h forecasting, *R* is equal to 0.956 and *MSE* is equal to 0.4369; while for one-hour forecasting, *R* = 0.928 and *MSE* = 0.48454. Figure 7 shows the forecasting error distribution for 0.5 and one hour. It shows that about 90% of the forecasting error are less than 1 °C.

Figures 8 and 9 shows the forecasting results at two and four hours. We observe a deterioration in the quality of forecasting regarding those obtained at 0.5 and one hour. For two-hour forecasting, *R* = 0.9109 and *MSE* = 0.89078, while for four-hour forecasting, *R* = 0.8370 and *MSE* = 1.23783. Figure 10 shows the forecasting error distribution for two and four hours. It shows that for the former, about 70% of the forecasting error are less than 1 °C, while for the latter about 64% of the forecasting error are less than 1 °C. Table 5 summarizes the forecasting results.
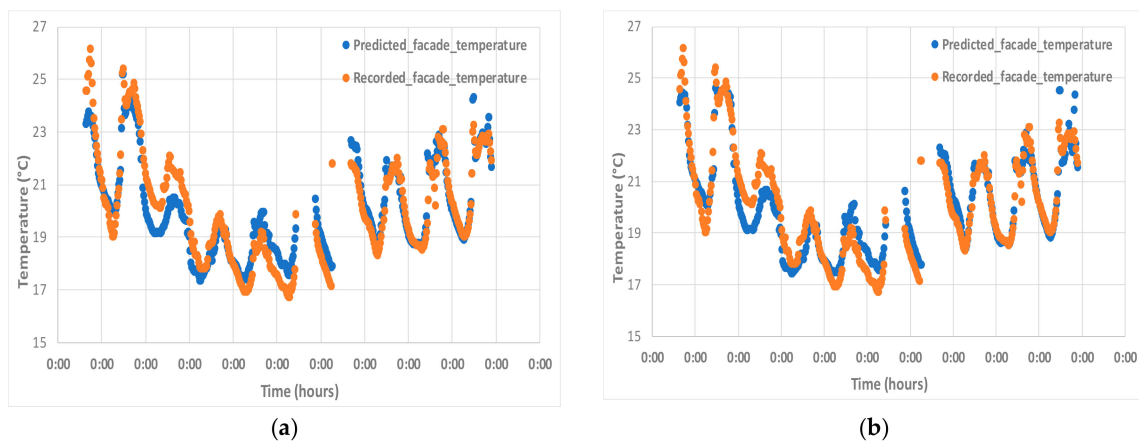
Figure 5. Recorded and predicted facade temperature variation in the time domain: (**a**) prediction for 0.5 h; and (**b**) prediction for 1 h.
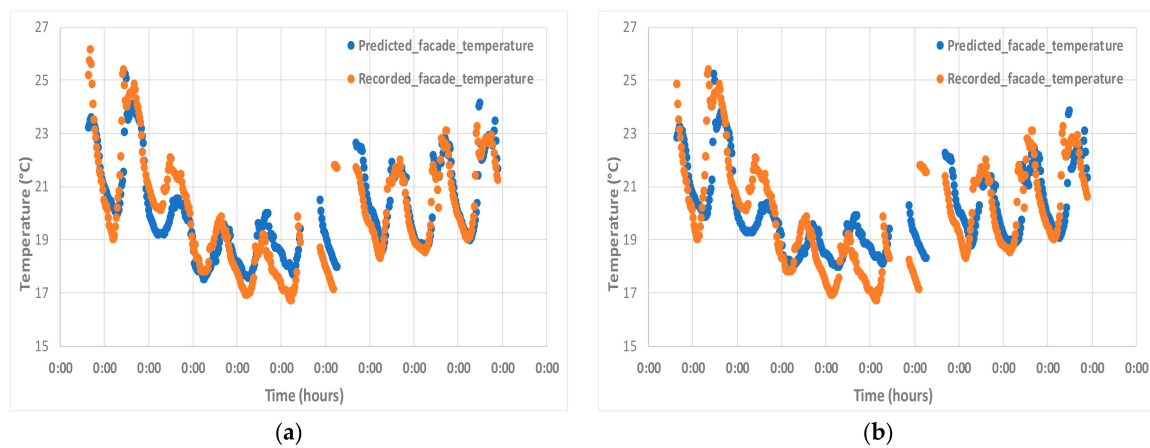

Figure 6. Predicted facade temperature with the recorded facade temperature (input parameter = outdoor temperature): (**a**) prediction for 0.5 h; and (**b**) prediction for 1 h.
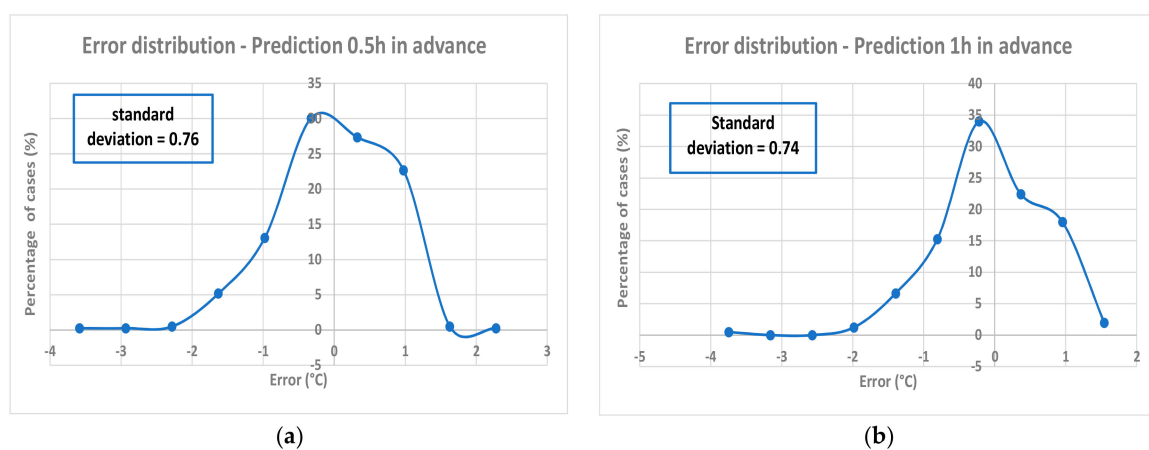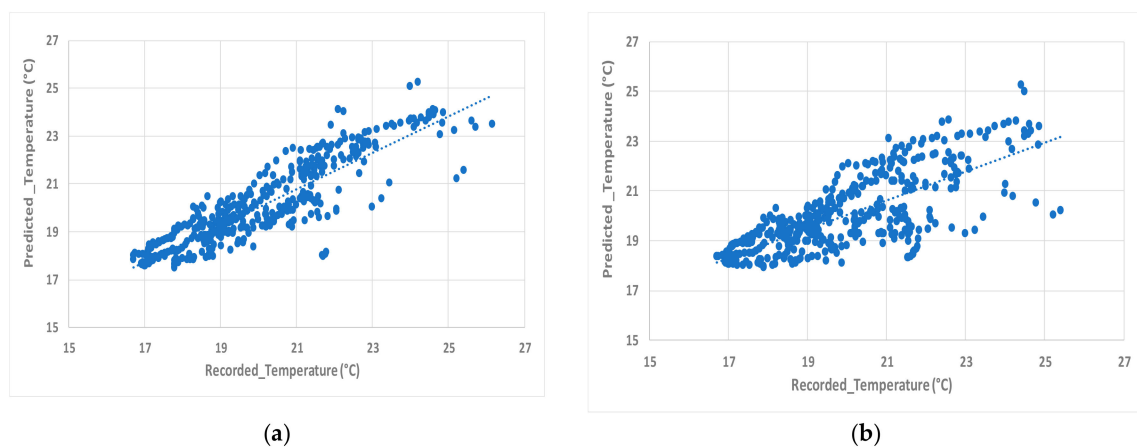

Figure 7. Distribution of the error forecasting (input parameter = outdoor temperature): (**a**) prediction for 0.5 h; and (**b**) prediction for 1 h.
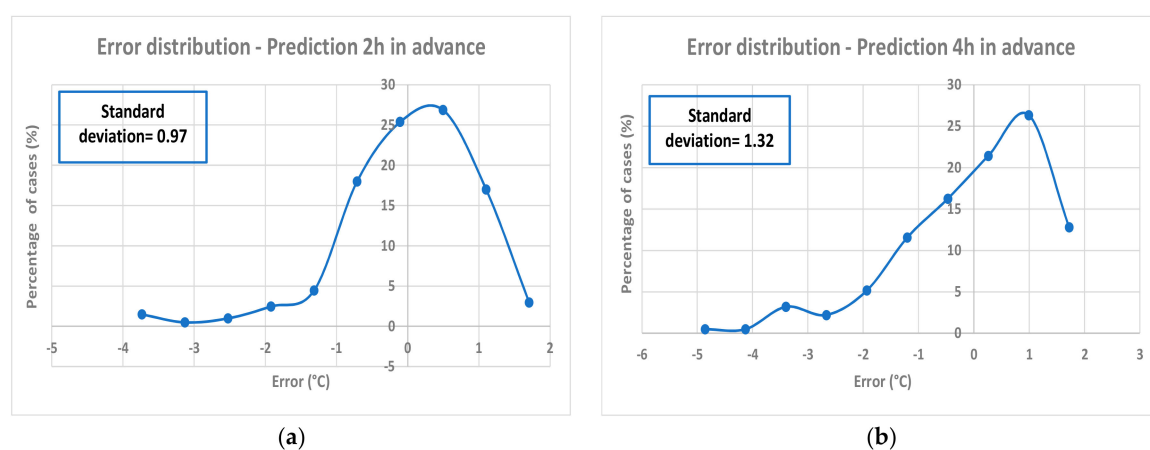
Figure 8. Recorded and predicted facade temperature variation in the time domain: (**a**) prediction for 2 h; (**b**) prediction for 4 h.

Figure 9. Predicted facade temperature with the recorded facade temperature (input parameter = outdoor temperature): (**a**) prediction for 2 h; and (**b**) prediction for 4 h.

Figure 10. Distribution of error forecasting (input parameter = outdoor temperature): (**a**) prediction for 2 h; and (**b**) prediction for 4 h.
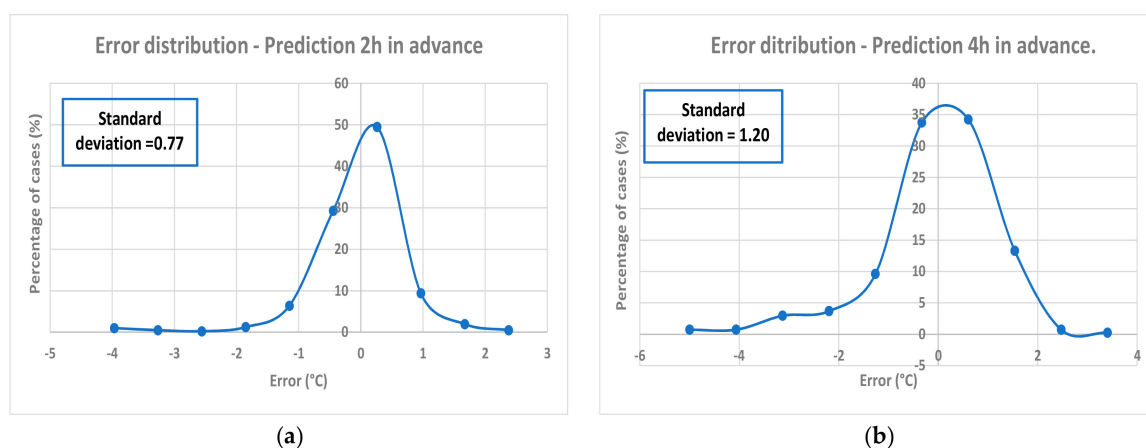
Table 5. Performances of the forecasting models (input parameter = outdoor temperature)

Model	Time	*R*	*MSE*
1	+0.5 h	0.9560	0.436900
2	+1 h	0.9528	0.484594
3	+2 h	0.9109	0.89078
4	+4 h	0.8370	1.23783

4.2.2. Use of the Outdoor Temperature and the History of the Facade Temperature as Input Parameters

In this section, both outdoor temperature and three-hour facade temperature history are used as input parameters in the forecasting model. The forecasting model provides the temperature at 0.5, 1, 2, and 4 h. Table 6 summarizes the obtained results. The temperature forecasting is improved regarding the forecasting model using the outdoor temperature as input. This result is particularly interesting for the temperature foresting at two hours: $R = 0.957$ and $MSE = 0.3299$ to be compared with $R = 0.9109$ and $MSE = 0.89078$ obtained with the outdoor temperature as input parameter. Figure 11 shows the forecasting error distribution for two hours. It shows that about 88% of the forecasting error are less than 1 °C to be compared with 70% obtained with the previous model.

The four-hour foresting is still weak with $R = 0.852$; $MSE = 1.0533$. About 68% of the forecasting error are less than 1 °C (Figure 11).

(**a**)　　　　　　　　　　　(**b**)

Figure 11. Distribution of error forecasting (input parameter = outdoor temperature and 3-h facade temperature): (**a**) prediction for 2 h; and (**b**) prediction for 4 h.

Table 6. Performances of the forecasting models (input parameters = outdoor temperature and three-hour facade temperature)

Model	Time	*R*	*MSE*
1	+0.5 h	0.992	0.0701
2	+1 h	0.982	0.1515
3	+2 h	0.957	0.3299
4	+4 h	0.852	1.0533

4.3. Indoor Temperature Forecasting (Room Center)

The ANN approach is used for forecasting the temperature at the room center considering only the facade temperature as input parameter. Figure 12 shows a comparison of 'predicted' and 'recorded' indoor temperatures. A good agreement is observed between recorded temperature and ANN prediction with $R = 0.951$; $MSE = 0.1679$. Only 1% of data has an error greater than 1 °C (Figure 13).

(**a**)

(**b**)
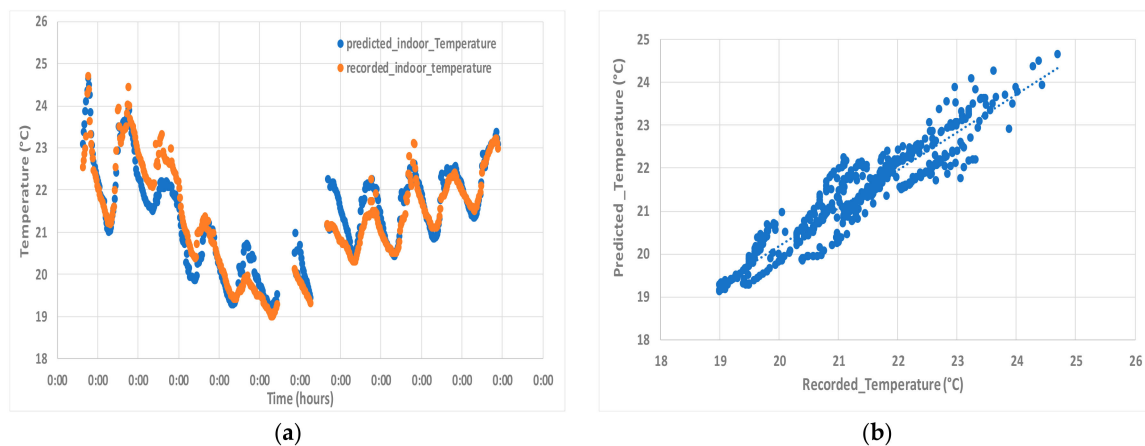
Figure 12. Predicted and recorded indoor temperatures: (**a**) the variation of both temperatures in time domain; and (**b**) the predicted indoor temperature with the recorded indoor temperature.
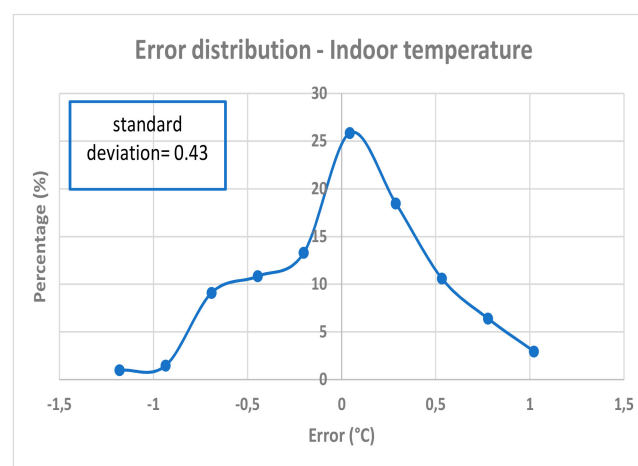
Figure 13. Distribution of error forecasting for indoor temperature (input parameters = facade temperature).

5. Discussion of Results

Relevance analysis and ANN modeling using different sets of input parameters showed that the indoor temperature forecasting could be conducted with good precision considering only outdoor temperature and indoor facade temperature history. Indeed, the influence of solar radiation, humidity, and outdoor temperature history in the forecasting model could be neglected. The prediction of the facade temperature was conducted with different inputs parameters and for different forecasting times. In the example presented in this paper, predictions were good up to two hours. The four-hour prediction gave unsatisfactory results with $R = 0.852$; $MSE = 1.0533$.

Indoor temperature forecasting was successfully conducted using the facade temperature. Available data did not include indoor activities. The presence of significant indoor activities—such as meetings, use of energy consuming devices, as well as opening doors and windows—could significantly affect the energy balance in the room. If these activities are significant, they should be monitored and included in the forecasting model.

6. Conclusions

This paper proposed a methodology for the development of a simplified ANN-based model for forecasting indoor temperature. The methodology includes two steps. The first step concerns the

forecasting of the indoor facade temperature considering outdoor and indoor conditions, while the second step concerns the prediction of the temperature at the room center considering only the indoor facade temperature.

This paper shows that both relevance analysis and the use of different sets of input parameters could lead to a simplified forecasting model with restricted input parameters. This methodology was illustrated through its application to data collected in an old building. Data included outdoor and indoor temperature and humidity, as well as solar radiation. Analyses showed that two-hour facade temperature forecasting could be conducted with good precision using only the outdoor temperature and three-hour facade temperature history. This result could not be generalized. However, the proposed methodology could be used for other situations by using first only temperature sensors for measuring the outdoor and the indoor facade temperatures. Concerning the second step, the ANN model gave good forecasting of the temperature at the room center in considering only the facade temperature. Available data did not include indoor activities. The presence of significant indoor activities should be considered in the forecasting model.

Author Contributions: Nivine Attoue and Isam Shahrour conceived and designed the experiments; Nivine Attoue performed the experiments; Nivine Attoue, Isam Shahrour and Rafic Younes analyzed the data; Nivine Attoue and Isam Shahrour wrote the paper.

Conflicts of Interest: The authors declare no conflict of interest.

References

1. Holz, R.; Hourigan, A.; Sloop, R.; Monkman, P.; Krarti, M. Effects of standard energy conserving measures on thermal comfort. *Build. Environ.* **1997**, *32*, 31–43. [CrossRef]
2. Tham, K.W.; Ullah, M.B. Building energy performance and thermal comfort in Singapore. *ASHRAE Trans.* **1993**, *99*, 308–321.
3. Huebner, G.M.; McMichael, M.; Shipworth, D.; Shipworth, M.; Durand-Daubin, M.; Summerfield, A. The reality of English living rooms, a comparison of internal temperatures against common model assumptions. *Energy Build.* **2013**, *66*, 688–696. [CrossRef]
4. Nguyen, J.L.; Schwartz, J.; Dockery, D.W. The relationship between indoor and outdoor temperature, apparent temperature, relative humidity and absolute humidity. *Indoor Air* **2014**, *24*, 103–112. [CrossRef] [PubMed]
5. Hens, H.; Parijs, W.; Deurinck, M. Energy consumption for heating and rebound effects. *Energy Build.* **2010**, *42*, 105–110. [CrossRef]
6. Shao, X.; Ma, X.; Li, X.; Liang, C. Fast prediction of non-uniform temperature distribution: A concise expression and reliability analysis. *Energy Build.* **2017**, *141*, 295–307. [CrossRef]
7. Ruano, A.E.; Crispim, E.M.; Conceição, E.Z.E.; Lucio, M.M.J.R. Prediction of building's temperature using neural networks models. *Energy Build.* **2006**, *38*, 682–694. [CrossRef]
8. Fang, P.; Liu, T.; Liu, K.; Zhang, Y.; Zhao, J. A Simulation model to calculate temperature distribution of an air-conditioned room. In Proceedings of the 2016 8th International Conference on Intelligent Human-Machine Systems and Cybernetics, Hangzhou, China, 27–28 August 2006.
9. Jigang, Z. *Study on the Airflow & Temperature Field Characteristics in the Room with Wall Air Conditioner and on the Human Thermal Comfort*; Shandong University: Jinan, China, 2007.
10. Funahashi, K. On the approximate realization of continuous mappings by neural networks. *Neural Netw.* **1989**, *2*, 183–192. [CrossRef]
11. Hornik, K.; Stinchcombe, M.; White, H. Multilayer feed forward networks are universal approximators. *Neural Netw.* **1989**, *2*, 359–366. [CrossRef]
12. Girosi, F.; Poggio, T. Networks and the Best Approximation Property. *Biol. Cybern.* **1990**, *63*, 169–176. [CrossRef]
13. Soleimani-Mohseni, M.; Thomas, B.; Fahlén, P. Estimation of operative temperature in buildings using artificial neural network. *Energy Build.* **2006**, *38*, 635–640. [CrossRef]

14. Lu, T.; Viljanen, M. Prediction of indoor temperature and relative humidity using neural network models: Model comparison. *Neural Comput. Appl.* **2009**, *18*, 345–357. [CrossRef]

15. Zabada, S.; Shahrour, I. Analysis of Heating Expenses in a Large Social Housing Stock Using Artificial Neural Networks. *Energies* **2017**, *10*, 2086. [CrossRef]

16. Aljer, A.; Loriot, M.; Shahrour, I.; Benyahya, A. Smart system for social housing monitoring. In Proceedings of the 2017 Sensors Networks Smart and Emerging Technologies (SENSET), Beirut, Lebanon, 12–14 September 2017; IEEE: Piscataway, NJ, USA, 2017. [CrossRef]

17. Attoue, N.; Shahrour, I.; Younes, R.; Aljer, A.; Loriot, M. Analysis of Buildings Energy Losses Using Smart Monitoring. In Proceedings of the International Work-Conference on Time Series (ITISE 2017), Granada, Spain, 18–20 September 2017.

18. Khayatian, F.; Sarto, L.; Dall'O, G. Application of neural networks for evaluating energy performance certificates of residential buildings. *Energy Build.* **2016**, *125*, 45–54. [CrossRef]

19. Mba, L. *Modélisation du Comportement Thermique du Bâtiment: Application d'une Méthode Neuronale*; Université de Douala-Cameroun: Douala, Cameroon, 2009.

20. Mba, L.; Kemajou, A.; Meukam, P. Application of artificial neural network for modeling the thermal behavior of building in humid region. Presented at the Actes des 3ème Rencontres EG@, Yaoundé, Cameroun, 14–16 Septembre 2010.

21. Brano, V.L.; Ciulla, G.; Falco, M.D. Artificial neural networks to predict the power output of PV panel. *Int. J. Photoenergy* **2014**, *2014*, 193083. [CrossRef]

22. Kemajou, A.; Mba, L.; Meukam, P. Application of artificial neural network for predicting the indoor air temperature in modern building in humid region. *Br. J. Appl. Sci. Technol.* **2012**, *2*, 23–34. [CrossRef]

23. Manssouri, T.; Sahbi, H.; Manssouri, I.; Boudad, B. Utilisation d'un modèle hybride base sur la rlms et les rna-pmc pour la prédiction des paramètres indicateurs de la qualité des eaux souterraines cas de la nappe de Souss-Massa-Maroc. *Eur. Sci. J.* **2015**, *11*, 35–46.

24. Paudel, S.; Elmtiri, M.; Kling, W.L.; Le Corre, O.; Lacarrière, B. Pseudo dynamic transitional modeling of building heating energy demand using artificial neural network. *Energy Build.* **2014**, *70*, 81–93. [CrossRef]

25. Tasadduq, I.; Rehman, S.; Bubshait, K. Application of neural networks for the prediction of hourly mean surface temperatures in Saudi Arabia. *Renew. Energy* **2002**, *25*, 545–554. [CrossRef]

26. Said, S.M. Degree-day base temperature for residential building energy prediction in Saudia Arabia. *ASHRAE Trans.* **1992**, *98*, 346–353.

27. Ding, Y.; Zhang, Q.; Yuan, T.; Yang, K. Model input selection for building heating load prediction: A case study for an office building in Tianjin. *Energy Build.* **2018**, *159*, 254–270. [CrossRef]

28. Ferrari, S. Building envelope and heat capacity: Re-discovering the thermal mass of winter energy savings. In Proceedings of the 28th AIVC Conference, Crete, Greece, 27–29 September 2007.

29. Gagliano, A.; Patania, F.; Nocera, F.; Signorello, C. Assessment of the dynamic thermal performance of massive buildings. *Energy Build.* **2014**, *72*, 361–370. [CrossRef]

30. Ulgen, K. Experimental and theoretical investigation of effects of walls' thermos-physical properties on time lag and decrement factor. *Energy Build.* **2002**, *34*, 273–278. [CrossRef]